Materials Science & Engineering B 236–237 (2018) 70–75

Contents lists available at ScienceDirect

Materials Science & Engineering B

journal homepage: www.elsevier.com/locate/mseb

Production of carbon fibers through Forcespinning® for use as anode materials in sodium ion batteries

David Flores, Jahaziel Villarreal, Jorge Lopez, Mataz Alcoutlabi*

Department of Mechanical Engineering, University of Texas Rio Grande Valley, Edinburg, TX 78539, United States

ARTICLE INFO

Keywords:
Forcespinning
Sodium-ion battery
Carbon microfibers
Anode

ABSTRACT

We report results on the Forcespinning (FS) of Polyvinylpyrrolidone (PVP) solutions for the preparation/fabrication of carbon fibers (CFs) as anodes for sodium ion batteries (SIBs). The objective of this study is to manipulate the microstructure of the CFs to improve the intercalation kinetics of the sodium ion into the CF structure. The as prepared CFs were porous with an average fiber diameter of 1.99 μm. The electrochemical performance of the CF anodes was investigated by carrying out galvanostatic charge/discharge and impedance experiments on Na^+ half cells. The results show that the CF anodes exhibited a high discharge capacity of 330 mAh g^{-1} at the first discharge (Sodium insertion) and reversible capacity of 88 mAh g^{-1} after 100 cycles at a current density of 100 mA g^{-1}. The results are promising and show that Forcespun CFs are a stepping stone for anode materials in SIBs.

1. Introduction

Decades have passed since Sony first commercialized the lithium-ion battery (LIB) in 1991, but its long cycle life and high energy density characteristics have allowed LIBs to remain the most prominent secondary energy source in applications such as portable electronics and electric vehicles [1–4]. However, rising issues with LIBs including cost and finite amount of lithium from the world's reserve have paved the way for extensive research for alternatives [5] to lithium. Sodium ion batteries (SIBs) have received a great deal of attention as an alternative secondary energy source that circumvents the aforementioned issues with LIBs. Due to the widespread availability of sodium and its similarities with lithium, such as its conductive property, SIBs become inexpensive and more feasible option for large-scale energy storage applications such as electrical energy storage systems [6–8]. However, SIBs suffer from reduced energy density and inadequate cycling stability severely limiting its advancement into being the leading secondary energy source for large-scale applications. For these reasons, the development of stable anode materials that demonstrate improved performance of SIBs is essential and still ongoing.

A major drawback that arises when identifying an appropriate anode material for SIBs is the large radius of sodium (i.e. Na^+ ~ 1.09 Å) thus making it difficult to intercalate the sodium ion into the host material [9]. Several materials have been recently investigated for use as anodes in SIBs such as Na alloys (e.g. Sn, Sb, SnSb, P, etc.) and some conversion materials such as transition metal oxides, transition metal sulfide, etc. [10–13]. Hard carbon is also a material that has been considered as anode materials for SIBs. Hard carbons a disordered structure with wide interlayer distances that have proven to be beneficial for sodium storage. However, the major issue with the transition metal composites and hard carbons is that they suffer from high-volume expansions resulting in electrode pulverization that could lead to electrical disconnection between particles within the SIBs [14,15]. To compensate for the volumetric expansion, the size and morphology can be manipulated to allow for more reaction sites within the transition metal composites and hard carbons. Therefore, the size reduction into the nanoscale and synthesizing porous/hollow morphologies result in the improved performance of SIBs [16]. Nanostructured carbon-based materials such as carbon nanotubes, graphene, nanowires and carbon nanofibers have been extensively used as alternative anode materials for LIBs and SIBs [17]. Carbon nanofibers are advantageous due to their flexibility and low cost and are easy to produce compared to other nanostructured based carbon materials [17,18].

In most cases, carbon fibers are produced using polyacrylonitrile (PAN) due to its high carbon content after heat treatment. However, the high cost of PAN has limited the use of carbon fibers in numerous applications. Transitioning into low cost water based polymers such as Poly(vinyl alcohol) (PVA) and Polyvinylpyrrolidone (PVP) to produce CFs has proven to be an alternative method for the synthesis of CFs and

* Corresponding author.
E-mail address: mataz.alcoutlabi@utrgv.edu (M. Alcoutlabi).

https://doi.org/10.1016/j.mseb.2018.11.009
Received 23 September 2017; Received in revised form 13 October 2018; Accepted 22 November 2018

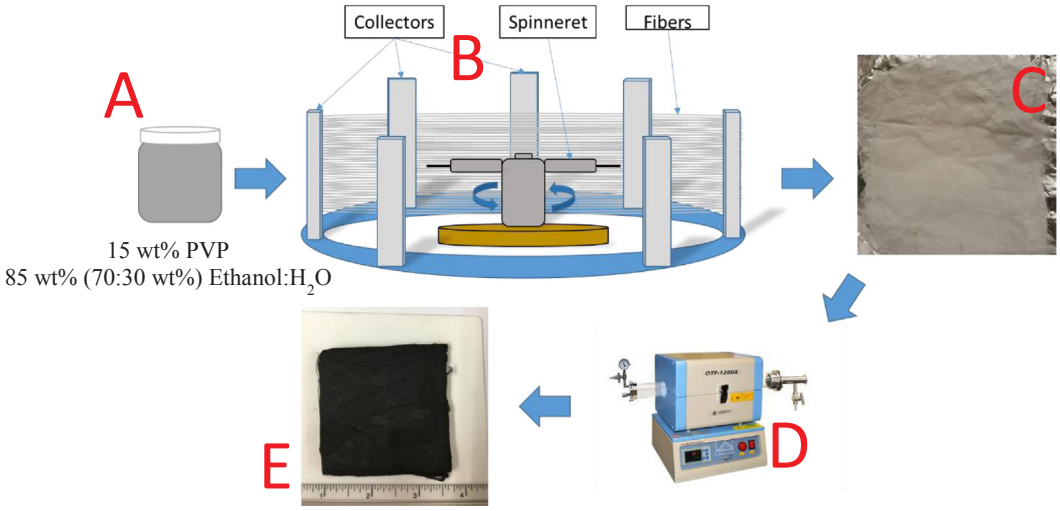

Fig. 1. The experimental procedure involved in producing CMFs. A PVP precursor solution (A) is Forcespun and collected (B) into a polymer precursor mat (C). The precursor mat is carbonized (D) to form the carbon fiber mat (E).

paved the way in the production of inexpensive carbon fiber/carbon fiber composites [19].

Increasing the surface area to volume ratio of the electrode material is one method used to improve the electrochemical performance of SIBs and LIBs. The development of nanostructured and binder-free anodes such as nanofibers, nanotubes, or nanowires has proven to increase the surface area to volume ratio and minimize the volume-expansion, thus, improving the energy density and specific power of SIBs [20]. Removing the need for non-conductive binders also increases the potential to load more active material that could lead to the overall performance increase of SIBs by eliminating some of the limiting factors associated with the binder material and by extension, increasing the overall flexibility of the electrode [21,22].

Herein, polymer precursor fibers were prepared via the Forcespinning® (FS) method and subsequently thermally treated to yield binder-free carbon microfibers (CMFs) for use as anodes in SIBs. The Forcespinning® method has previously been used by our group to fabricate binder-free anodes for lithium-ion batteries (LIBs) [1,2,23,24]. The Forcespinning® method consists of applying centrifugal forces to a polymer solution to overcome its surface tension, thus forcing the polymer solution to exit the spinneret orifice resulting in the production of microfibers. The centrifugal forces are developed or generated or other word by applying rotational speeds of up to 20,000 rpm to the spinneret. This method of fabrication has a high fiber yield when compared to electrospinning and also provides a safer working environment, without the need of high voltages [25]. Other processing methods have been also used to produce carbon fibers for use in sodium ion batteries including the in-house built centrifugal spinning and electrostatic spinning [26,27]. The morphology and formation of fibers prepared by these two methods are very different from those prepared by Forcespinning [24,28]. In fact, the in-house built centrifugal spinning cannot be used to produce fibers at high rotational speeds and it has no capacity of melt spinning [29]. The Forcespinning method on the other hand can produce fibers from solution precursors at a high speed up to 12,000 rpm with the capability of melt spinning at up to 25,000 rpm [30]. In this work, the FS method is used to produce polymer precursor fibers from PVP polymer solutions in a binary solvent system of ethanol and water. These fibers are then subjected to thermal treatment in an argon atmosphere to produce the binder-free flexible CMFs that are directly employed as the anode material in SIBs. To the best of our knowledge, this is the first time ever to report results on the Forcespinning of PVP/(water/ethanol) precursor solution for use as carbon fibers in Sodium ion batteries.

2. Experimental

2.1. Material

Poly(vinylpyrrolidone) (PVP) with an average molecular weight (Mw) of 1,300,000 was purchased from Sigma-Aldrich USA. Absolute Ethanol (200 proof) and HPLC Grade Submicron Filtered Water were both purchased from Fisher Scientific. The Sodium cubes in mineral oil and Sodium Perchlorate ($NaClO_4$) were purchased from Sigma-Aldrich USA. Finally, the ethylene carbonate (EC) and dimethyl carbonate (DMC) were purchased from MTI Corp. USA.

2.2. Preparation of carbon fibrous mats

The polymer precursor was prepared by magnetically stirring 15 wt % PVP in 85 wt% solvent (70:30 wt% Ethanol:H_2O) for 24 h. The as-prepared polymer precursor solution was used to produce polymer precursor fibers via Forcespinning®. In Forcespinning®, high spinneret rotational speeds of up to 20,000 rpm generates centrifugal forces that allow for the formation of fiber jets at the tips of the needles. Initially, 1.5 mL of the prepared solution is injected into the spinneret affixed with two 30-gauge half-inch regular bevel needles. The rotational speed of the spinneret was maintained at 8000 rpm for 2 min until the solution was finished. After each run, the polymer precursor fibers were collected using a 4-in by 4-in cardboard square covered with spun-bond polypropylene substrate. The square is used to remove the fibers from the collectors as shown in Fig. 1B. Also in Fig. 1C depicts the fibrous mat after the fibers have been successfully removed from the polypropylene substrate. The fibrous mat is then dried at 120 °C in a vacuum oven for 16 h prior to heat treatment. The thermal treatment consisted of stabilization in air at 200 °C followed by carbonization at 435 °C (a heating rate of 2 °C/min was used throughout) in an argon atmos.

2.3. Electrochemical performance evaluation

The carbon fibers were used as free-standing anodes whose electrochemical performance was studied using a half-cell configuration of the 2032 cells. The free-standing carbon fiber anodes had a weight ranging between 2 and 8 mg. These masses were used to determine the current density and specific capacities of the Na^+ half cells. Sodium metal chips were used as the counter electrode, while glass microfibers were used as the separator. The electrolyte used consisted of a 1 M $NaClO_4$ salt in ethylene carbonate (EC)/dimethyl carbonate (DMC) (1:1 v/v) solvent. The coin cells were assembled in a high purity argon-filled

glove box (Mbraun, USA) with O_2 and H_2O concentrations of < 0.5 ppm. The LANHE CT2001A battery testing system was used to conduct galvanostatic charge–discharge experiments to assess the electrochemical performance of the Na^+ half-cells at a current density of 100 mA g^{-1} between 0.01 and 2.5 V. Cyclic voltammetry tests were performed by the Bio-Logic BCS-810 with a scan rate of 0.1 mV s^{-1}, and electrochemical impedance experiments were performed using the Autolab 128N with low and high frequencies of 0.1 Hz and 100 kHz, respectively. Finally, rate performance tests were evaluated at various current densities of 50, 100, 200, 400, and 500 mA g^{-1}. After the final test at a current density of 500 mA g^{-1}, the recovery capabilities of the carbon fiber anodes were assessed by decreasing the current density to its initial value of 50 mA g^{-1}.

3. Results and discussion

3.1. Morphology and fiber diameter distribution

Scanning Electron Microscopy (Zeiss ΣIGMA VP) was used to analyze the morphology of the carbon fibers and AxioVision LE (Zeiss) was used to measure the fiber diameters. It has been previously shown that solution properties, such as polymer content and Forcespinning parameters (rotational speed) can affect the overall fiber diameter [31]. The resulting measurements are depicted in the fiber diameter distribution curve (histogram) (Fig. 3), that result from rotational speeds of 8000 rpm with a 15% polymer concentration. Fig. 2A and B shows the morphology of the carbon fibers. After calcination, the carbon fibers showed a smooth surface maintaining a solid cross-section.

Also, Fig. 3 shows the histogram and it is observed that many of the fibers have a diameter in the range of 1.8–2.4 μm with the average fiber diameter being 1.99 μm, proving that the carbon fibers produced via Forcespinning® are considered carbon microfibers (CMFs). Since reducing the size of active materials is an efficient way to tackle high volume change problems introduced by the sodiation and desodiation processes [16], the size of the CMFs can be an attributing factor to some of the loss that the sodium anodes suffered during cycling.

3.2. Raman spectra

The Forcespun CMF's structure was investigated by Raman spectroscopy which was evaluated with the Bruker Senterra Raman Microscope. Fig. 4 shows the Raman spectra results for the CMFs; more specifically, the characteristic D-band and G-band peaks at 1361 cm^{-1} and 1585 cm^{-1} respectively [32]. The D-band peak is representative of the disordered sp^2 phase whereas the G-band peak defines the bond stretching of all pairs of sp^2 atoms in rings and chains [33]. The degree of disorder is defined by the R-value, calculated from a ratio between the intensity of the D-band to G-band peaks. The higher the R-value is, the more disordered the carbon structure is [32,33]. In this case, the R-value is approximately 1.7 meaning that the structure of the CMFs is highly disordered. The highly disordered structure can accommodate some of the volume expansions that these hard carbons undergo during cycling as well as increase the amount of sodium that can be stored within the anode material.

4. Electrochemical analysis

4.1. Electrochemical performance

To evaluate the electrochemical performance of the CMF anodes, cycling performance tests were carried out on Na^+ half-cells at a current density of 100 mA g^{-1} over 100 cycles. Fig. 5 depicts the sodiation (charge)/desodiation (discharge) curves of the CMF anodes. These charge/discharge curves were obtained by testing over a potential window of 0.01–2.5 V at a constant current density of 100 mA g^{-1}. At the first discharge cycle (sodium insertion), the CMFs show an initial capacity of 330 mAh g^{-1}. However, the charge capacity (sodium deinsertion) at the first cycle of the CMFs is 106 mAh g^{-1} indicating a loss in capacity over one-third of its capacity which is mostly due to the formation of the Solid Electrolyte Interphase (SEI) layer. This can lead

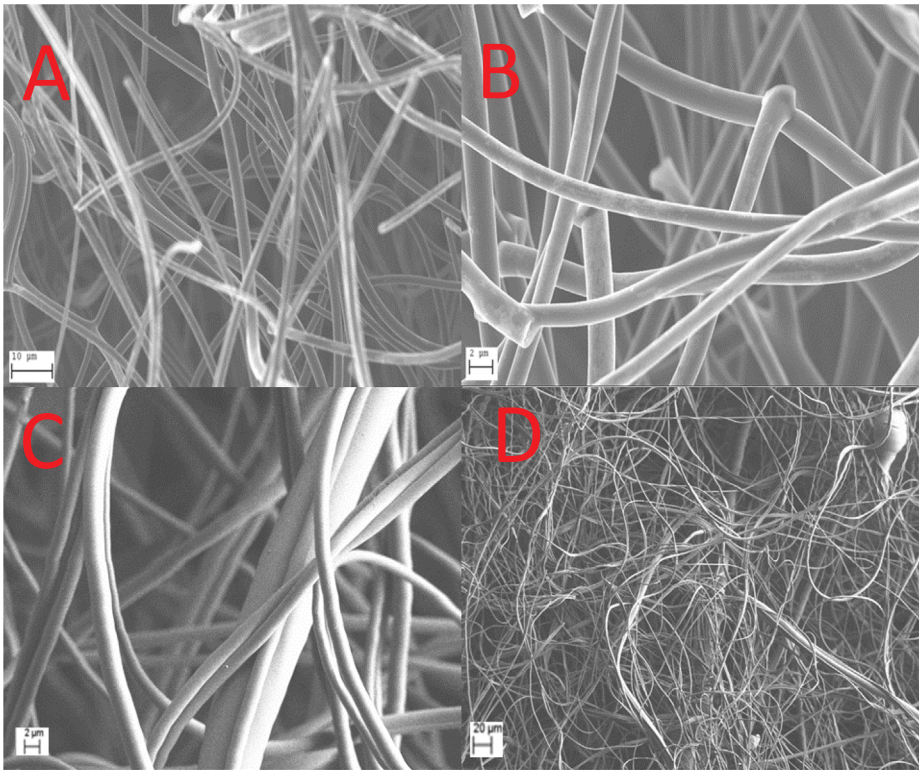

Fig. 2. SEM images of the CMFs (A, B) and of the polymer precursor fibers (C, D).

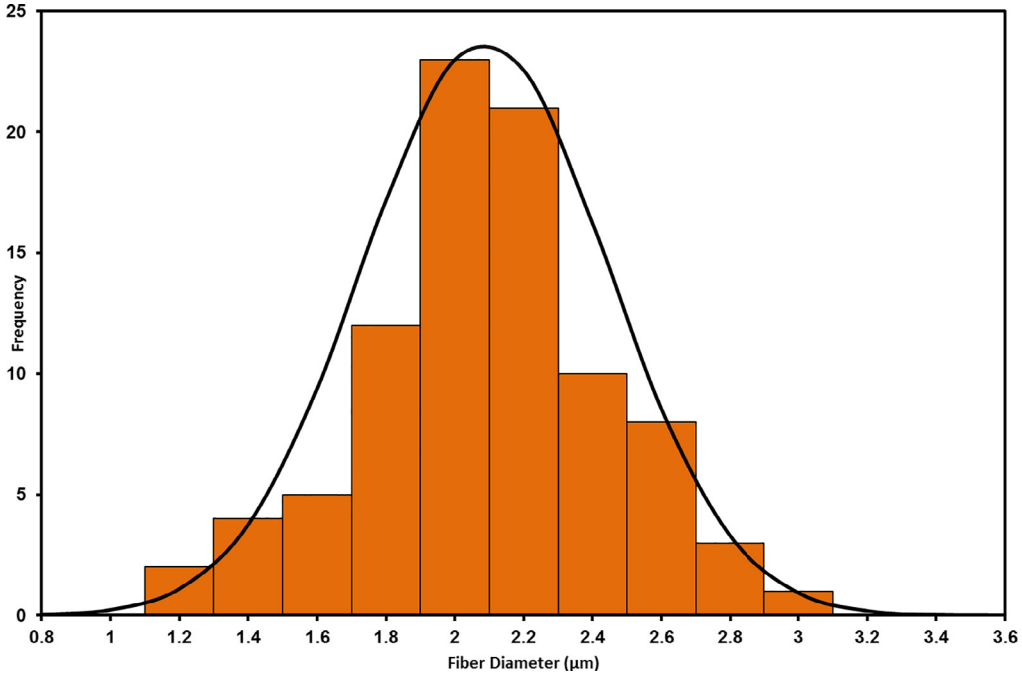

Fig. 3. Fiber diameter distribution of the CMFs.

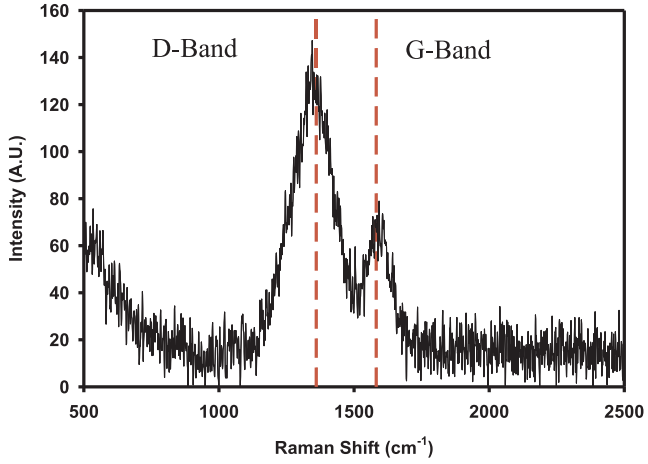

Fig. 4. Raman spectra of the CMFs conducted with the Bruker spectra.

to a hindrance in the electrical contact between the sodium and the CMF anode. This hindrance makes the intercalation and deintercalation of sodium ions during the sodiation and desodiation processes increasingly difficult, ultimately leading the CMFs to show a 100th cycle capacity of 88 mAh g^{-1}.

In fact, the formation of SEI layer on the anode surface in LIBs [34] is more stable than that formed in SIBs [35]. Metallic sodium anodes corrode continuously in the presence of organic electrolytes where a stable SEI cannot be formed [36]. This has been a drawback for the development of high energy density SIBs with suitable anode material and optimized electrolyte compositions. Unlike Li metal, metallic Na-anode exhibits more dendrite formation than Li and has lower melting temperature which makes it difficult to use as metallic NA-anode in SIBs. The most important parameter affecting the reversible capacity in SIBs is the SEI formation at the first cycle. The formation of a SEI passivation layer on the electrode surface in SIBs is more difficult than that in LIBs due to the higher solubility of the decomposed products in sodium-based electrolytes compared to that in Li-based electrolytes [37]. This is mainly caused by Lewis acidity difference between Li and Na ions (i.e. higher for Li+ than for Na+). The formation of a stable

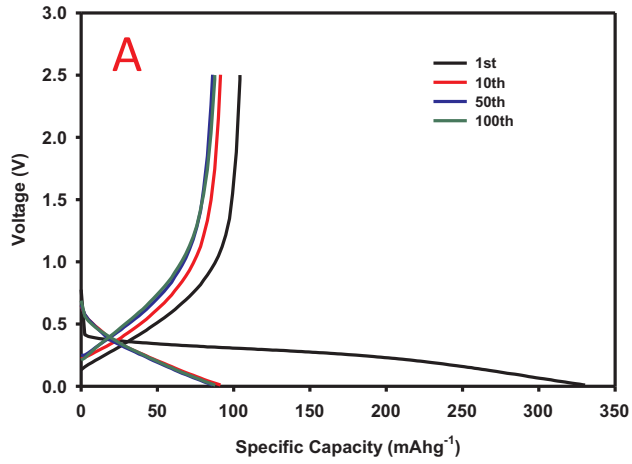

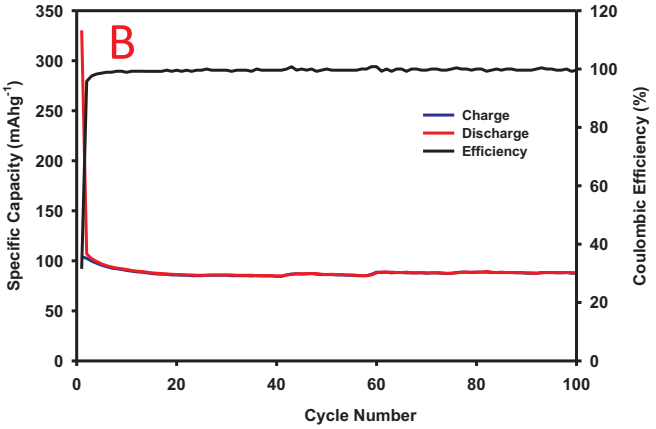

Fig. 5. Charge/discharge profiles (A) and cycle performance (B) of the CMF anodes.

SEI layer at the anode surface in SIBs is very crucial to prevent the electrolyte from further decomposition during prolonged charge/discharge cycles, thus resulting in high revisable capacity and long cycle life of the battery [38,39]. For example, the SEI layer formation on hard carbon electrode in SIBs was different from that on the same electrode in LIBs where thicker and homogenous SEI layer was observed for the LIB anode while the SEI layer formed on had carbon in SIBs was thinner (5–10 nm) and was inhomogeneous [40]. Different additives can be used to improve the SEI layer formation in LIBs while only one additive, Fluoroethylene carbonate (FEC), has been considered as an efficient additive in SIBs confirming the nature of SEI layer formation in LIBs and SIBs [41]. The most efficient electrolyte used in SIBs to stabilize the SEI layer formation in SIBs is $NaClO_2$ in Ethylene carbonate (EC):Propylene carbonate (PC) [42].

Fig. 5 also shows that the initial capacity loss results in the coulombic efficiency of the Na^+ half-cell to be ~32% the majority being due to the formation of the SEI layer. The low coulombic efficiency of the carbon fibers at the first cycle is caused by the high surface area to volume ratio of the fibers, the SEI layer formation at the first discharge cycle and by the porous structure of the fibers. Unlike electrospinning or sprayspinning, the Forcespinning of PVP fibers usually results in fibers that are porous due mainly the difference in vapor pressure between ethanol and water. Ethanol has higher vapor pressure than water and it tends to evaporate quickly during spinning, leaving water droplet in the PVP fiber matrix [43]. The high porosity of fibers results in high surface area and large SEI layer, thus high loss in capacity and low coulombic efficiency of the carbon fiber anode are observed at the first discharge/charge cycle (high irreversible capacity). Another potential reason for a minimal portion of the capacity loss would be the volume expansion suffered by hard carbons during the sodiation/desodiation processes. This can be deemed a minimal loss due to the highly disordered structure of the CMFs that is represented by the R-value in the Raman spectra (Fig. 4). Although the initial coulombic efficiency of the CMF anode is low, subsequent cycles show an excellent stable and high efficiency of ~99% as depicted in Fig. 5B.

The electrochemical performance of the CMFs was further evaluated by conducting current rate (or rate capability tests, rate performance test) experiments of the Na^+ half-cells at different current densities. The CMF anodes were cycled for 10 cycles at various current densities of 50, 100, 200, 400, 500 and then again at 50 mA g^{-1}. This will exemplify the CMF anodes' ability to perform at higher current densities as well as evaluate the capacity recovered after being cycled from a high to low current density. Fig. 6 depicts the rate performance of the CMF anodes showing desodiation capacities (charge) of 156, 80, 33, 18, and 10 mAh g^{-1} for current densities of 50, 100, 200, 400, and 500 mA g^{-1}, respectively. At higher current densities, the rate of sodiation and desodiation becomes overwhelming, resulting in low capacity. Although the capacity at higher current densities is low, the CMF anodes still recover to a capacity of 94 mAh g^{-1} at the final current density of 50 mA g^{-1}. The CMF anodes show ~60% recovery capability and excellent stability at each individual current density. This proves that CMF anodes are an excellent preliminary material for use in SIBs.

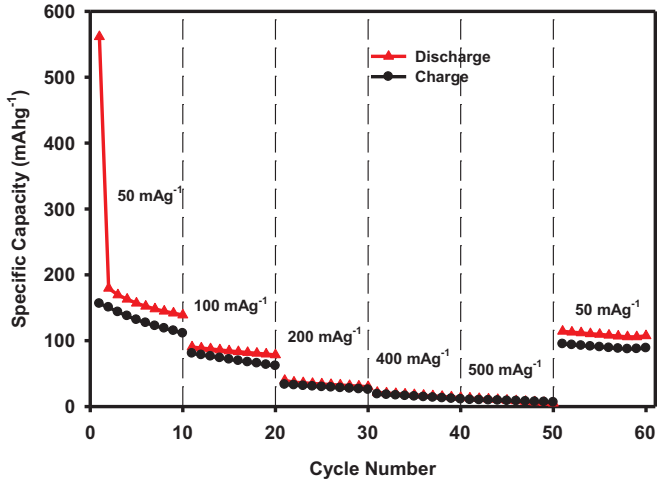

Fig. 6. Rate performance of the CMF anodes at 50, 100, 200, 400, and 500 mA g^{-1}.

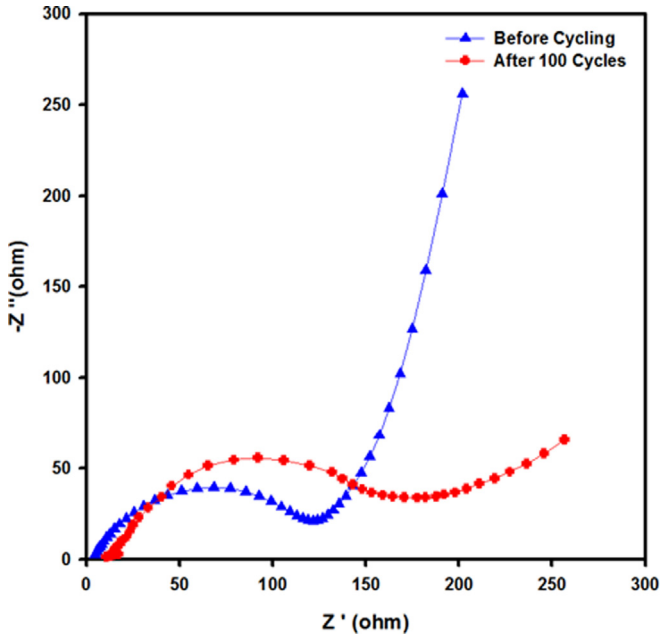

Fig. 7. Nyquist impedance plots for the fresh uncycled cells and the aged cycled cells.

4.2. Impedance

In order to investigate the electrochemical performance of the carbon fibers-anode further, electrochemical spectroscopy (EIS) experiments were conducted on sodium ion half-cells in the frequency range between 0.1 Hz and 100,000 Hz. The Nyquist plots for the electrochemical impedance before (fresh cell) and after cycling (aged cell) of the CMFs are shown in Fig. 7. The Nyquist plots of the CMFs before and after cycling show semicircles in the high and medium frequency range, followed by a sloping line in the low frequency region. The semicircles in the high to medium frequency region are associated with the resistance of the SEI layer (R_f) formed on the CMFs-electrode and with the resistance of the charge transfer (R_{ct}) at the electrode/electrolyte interface, respectively [44]. The straight line in the low frequency represents the diffusion properties of Na^+ within the carbon fibers-electrode.

As shown in Fig. 7, after 100 cycles, there is an increase in the diameter of the semi-circle indicating increases (i.e. from the shift to the right on the Z-real axis) in the resistance of the SEI layer and the charge transfer. The growth of the SEI passivating layer on the anode creates resistance to sodium ion flow, which results in an increase in the charge transfer resistance and the impedance of the anode [39,45]. In addition, the much longer low-frequency sloping line of CMFs-anode before cycling (fresh cell) is higher than that after 100 cycles (aged cell) indicating that the diffusion of sodium ions into the CMFs-anode is much faster for the fresh cell than that for the aged SIB cell. The increase in the charge transfer resistance, R_{ct}, after 100 cycles might be due to the loss of structural stability of CMFs-anode. Similar results were reported on the use $NiSe_2$ nanofibers as anodes in SIBs [46]. The lower charge transfer resistance of the CMF-anode before cycling (fresh cell)

indicates faster charge-transfer kinetics than that after 100 cycles. The increase in the overall electrochemical impedance of the CMFs-anode after 100 cycles, led to a negative effect on the sodium ion kinetics which correlates with the loss in capacity observed in Fig. 5A.

5. Conclusion

The CMFs exhibit an adequate cycling stability, maintaining $\sim 90\,mAh\,g^{-1}$ after 100 cycles at a current density of $100\,mA\,g^{-1}$. These preliminary results show that FS allows for the mass production of CMFs from PVP polymer precursor solutions in a green solvent mixture that show an acceptable stability and recovery capabilities as binder-free anodes for SIBs. The electrochemical performance of the CMFs shows a high irreversible capacity that come mostly comes from the formation of the SEI layer. There is ongoing work in our laboratory to try and minimize the loss by changing the morphology of the fiber, using electrolyte additives that have proven to produce and even SEI layer, as well as producing fibers from other polymers in a 100% water solvent solution.

Acknowledgements

This research is supported by National Science Foundation (USA) under PREM grant DMR; con1523577: UTRGV-UMN Partnership for Fostering Innovation by Bridging Excellence in Research and Student Success. This work was also supported by the USDA National Institute of Food and Agriculture (award #2015-38422-24059) for the Integrating Food Science/Engineering and Education Network (IFSEEN) program. We would also like to acknowledge Mr. Hilario Cortez for his assistance with the SEM and EDS analyses.

References

[1] V.A. Agubra, et al., A comparative study on the performance of binary SnO_2/NiO/C and Sn/C composite nanofibers as alternative anode materials for lithium ion batteries, Electrochim. Acta 224 (2017) 608–621.
[2] L. Zuniga, et al., Multichannel hollow structure for improved electrochemical performance of TiO_2/carbon composite nanofibers as anodes for lithium ion batteries, J. Alloy Compd. 686 (2016) 733–743.
[3] H. Kim, et al., Recent progress in electrode materials for sodium-ion batteries, Adv. Energy Mater. 6 (19) (2016) 1600943-n/a.
[4] Y. Lu, et al., Syntheses and energy storage applications of MxSy (M = Cu, Ag, Au) and their composites: rechargeable batteries and supercapacitors, Adv. Funct. Mater. 27 (44) (2017).
[5] M. Wang, et al., Sb nanoparticles encapsulated in a reticular amorphous carbon network for enhanced sodium storage, Small 11 (40) (2015) 5381–5387.
[6] H. Gao, et al., A sodium-ion battery with a low-cost cross-linked gel-polymer electrolyte, Adv. Energy Mater. 6 (18) (2016) 1600467-n/a.
[7] Shasha Zheng, H. Xue, Huan Pang, Supercapacitors based on metal coordination materials, Coord. Chem. Rev. 373 (15) (2018) 2–21.
[8] X.R. Li, et al., N, S co-doped 3D mesoporous carbon-$Co_3Si_2O_5(OH)(4)$ architectures for high-performance flexible pseudo-solid-state supercapacitors, J. Mater. Chem. A 5 (25) (2017) 12774–12781.
[9] L.P. Wang, et al., Recent developments in electrode materials for sodium-ion batteries, J. Mater. Chem. A 3 (18) (2015) 9353–9378.
[10] L. Ji, et al., Graphene-based nanocomposites for energy storage, Adv. Energy Mater. 6 (16) (2016) 1502159-n/a.
[11] M. Mortazavi, et al., High capacity group-15 alloy anodes for Na-ion batteries: electrochemical and mechanical insights, J. Power Sources 285 (2015) 29–36.
[12] V. Palomares, et al., Na-ion batteries, recent advances and present challenges to become low cost energy storage systems, Energy Environ. Sci. 5 (3) (2012) 5884–5901.
[13] S.S. Zheng, et al., Transition-metal (Fe Co, Ni) based metal-organic frameworks for electrochemical energy storage, Adv. Energy Mater. 7 (18) (2017).
[14] M. Dirican, X. Zhang, Centrifugally-spun carbon microfibers and porous carbon microfibers as anode materials for sodium-ion batteries, J. Power Sources 327 (2016) 333–339.
[15] A. Ponrouch, A.R. Goñi, M.R. Palacín, High capacity hard carbon anodes for sodium ion batteries in additive free electrolyte, Electrochem. Commun. 27 (2013) 85–88.
[16] Y. Zhu, et al., Electrospun Sb/C fibers for a stable and fast sodium-ion battery anode, ACS Nano 7 (7) (2013) 6378–6386.
[17] L.W. Ji, et al., Recent developments in nanostructured anode materials for rechargeable lithium-ion batteries, Energy Environ. Sci. 4 (8) (2011) 2682–2699.
[18] W.H. Li, et al., Carbon nanofiber-based nanostructures for lithium-ion and sodium-ion batteries, J. Mater. Chem. A 5 (27) (2017) 13882–13906.
[19] R. Nava, et al., Centrifugal spinning: an alternative for large scale production of silicon–carbon composite nanofibers for lithium ion battery anodes, ACS Appl. Mater. Interf. 8 (43) (2016) 29365–29372.
[20] H.-G. Wang, et al., Electrospun materials for lithium and sodium rechargeable batteries: from structure evolution to electrochemical performance, Energy Environ. Sci. 8 (6) (2015) 1660–1681.
[21] L. Wu, et al., Sb–C nanofibers with long cycle life as an anode material for high-performance sodium-ion batteries, Energy Environ. Sci. 7 (1) (2014) 323–328.
[22] L. Ji, et al., Controlling SEI formation on SnSb-porous carbon nanofibers for improved Na ion storage, Adv. Mater. 26 (18) (2014) 2901–2908.
[23] V.A. Agubra, et al., Composite nanofibers as advanced materials for Li-ion, Li-O_2 and Li-S batteries, Electrochim. Acta 192 (2016) 529–550.
[24] V.A. Agubra, et al., Forcespinning: a new method for the mass production of Sn/C composite nanofiber anodes for lithium ion batteries, Solid State Ion. 286 (2016) 72–82.
[25] K. Sarkar, et al., Electrospinning to Forcespinning™, Mater. Today 13 (11) (2010) 12–14.
[26] J.D. Zhu, et al., Nitrogen-doped carbon nanofibers derived from polyacrylonitrile for use as anode material in sodium-ion batteries, Carbon 94 (2015) 189–195.
[27] Y. Bai, et al., Mille-feuille shaped hard carbons derived from polyvinylpyrrolidone via environmentally friendly electrostatic spinning for sodium ion battery anodes, RSC Adv. 7 (9) (2017) 5519–5527.
[28] V.A. Agubra, et al., ForceSpinning of polyacrylonitrile for mass production of lithium-ion battery separators, J. Appl. Polym. Sci. 133 (1) (2016).
[29] F. Dabirian, S.A.H. Ravandi, A.R. Pishevar, The effects of operating parameters on the fabrication of polyacrylonitrile nanofibers in electro-centrifuge spinning, Fibers Polym. 14 (9) (2013) 1497–1504.
[30] N.E. Zander, Formation of melt and solution spun polycaprolactone fibers by centrifugal spinning, J. Appl. Polym. Sci. 132 (2) (2015).
[31] N. Obregon, et al., Effect of polymer concentration, rotational speed, and solvent mixture on fiber formation using Forcespinning®, Fibers 4 (2) (2016) 20.
[32] Y.-S. Ding, et al., Characteristics of graphite anode modified by CVD carbon coating, Surf. Coat. Technol. 200 (9) (2006) 3041–3048.
[33] Z. Li, J. Ding, D. Mitlin, Tin and tin compounds for sodium ion battery anodes: phase transformations and performance, Acc. Chem. Res. 48 (6) (2015) 1657–1665.
[34] E. Peled, The electrochemical-behavior of alkali and alkaline-earth metals in non-aqueous battery systems – the solid electrolyte interphase model, J. Electrochem. Soc. 126 (12) (1979) 2047–2051.
[35] M.A. Munoz-Marquez, et al., Na-ion batteries for large scale applications: a review on anode materials and solid electrolyte interphase formation, Adv. Energy Mater. 7 (20) (2017).
[36] M.D. Slater, et al., Sodium-ion batteries, Adv. Funct. Mater. 23 (8) (2013) 947–958.
[37] M. Dahbi, et al., Negative electrodes for Na-ion batteries, Phys. Chem. Chem. Phys. 16 (29) (2014) 15007–15028.
[38] D. Larcher, J.M. Tarascon, Towards greener and more sustainable batteries for electrical energy storage, Nat. Chem. 7 (1) (2015) 19–29.
[39] A. Bhide, et al., Electrochemical stability of non-aqueous electrolytes for sodium-ion batteries and their compatibility with $Na_{0.7}CoO_2$, Phys. Chem. Chem. Phys. 16 (5) (2014) 1987–1998.
[40] S. Komaba, et al., Electrochemical Na insertion and solid electrolyte interphase for hard-carbon electrodes and application to Na-ion batteries, Adv. Funct. Mater. 21 (20) (2011) 3859–3867.
[41] S. Komaba, et al., Fluorinated ethylene carbonate as electrolyte additive for rechargeable Na batteries, ACS Appl. Mater. Interf. 3 (11) (2011) 4165–4168.
[42] A. Ponrouch, A.R. Goni, M.R. Palacin, High capacity hard carbon anodes for sodium ion batteries in additive free electrolyte, Electrochem. Commun. 27 (2013) 85–88.
[43] T. Hou, et al., Highly porous fibers prepared by centrifugal spinning, Mater. Des. 114 (2017) 303–311.
[44] B.K. Guo, et al., Soft-templated mesoporous carbon–carbon nanotube composites for high performance lithium-ion batteries, Adv. Mater. 23 (40) (2011) 4661-+.
[45] V. Agubra, J. Fergus, Lithium ion battery anode aging mechanisms, Materials 6 (4) (2013) 1310–1325.
[46] J.S. Cho, S.Y. Lee, Y.C. Kang, First introduction of $NiSe_2$ to anode material for sodium-ion batteries: a hybrid of graphene-wrapped $NiSe_2$/C porous nanofiber, Sci. Rep. 6 (2016).